2014

Synthesis of Liquid Core–Shell Particles and Solid Patchy Multicomponent Particles by Shearing Liquids Into Complex Particles (SLICE)

Ian Tevis
Iowa State University, itevis@iastate.edu

Lucas B. Newcomb
University of Massachusetts Boston

Martin M. Thuo
Iowa State University, mthuo@iastate.edu

Langmuir

Article

pubs.acs.org/Langmuir

Synthesis of Liquid Core–Shell Particles and Solid Patchy Multicomponent Particles by Shearing Liquids Into Complex Particles (SLICE)

Ian D. Tevis,[†,‡] Lucas B. Newcomb,[†] and Martin Thuo*[,†,‡]

[†]Department of Chemistry, University of Massachusetts—Boston, 100 Morrissey Boulevard, Boston, Massachusetts 02125 United States

[‡]Materials Science and Engineering, Iowa State University, 2220 Hoover Hall, Ames, Iowa 50011 United States

Supporting Information

ABSTRACT: We report a simple method that uses (i) emulsion shearing with oxidation to make core–shell particles, and (ii) emulsion shearing with surface-tension driven phase segregation to synthesize particles with complex surface compositions and morphologies. Subjecting eutectic gallium–indium, a liquid metal, to shear in an acidic carrier fluid we synthesized smooth liquid core–shell particles 6.4 nm to over 10 μm in diameter. Aggregates of these liquid particles can be reconfigured into larger structures using a focused ion beam. Using Field's metal melts we synthesized homogeneous nanoparticles and solid microparticles with different surface roughness and/or composition through shearing and phase separation. This extension of droplet emulsion technique, SLICE, applies fluidic shear to create micro- and nanoparticles in a tunable, green, and low-cost approach.

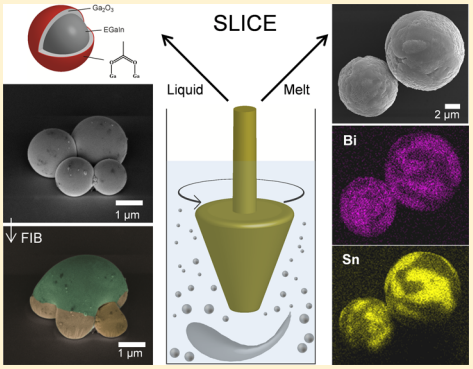

INTRODUCTION

There are two general methods for the preparation of complex particles: bottom-up and top-down. Nucleation and growth is a bottom-up method used to fabricate nanoparticles albeit with a limitation in the size and surface complexity.[1] Synthesis of colloidal particles with complex surface architectures and tunable layer thicknesses or compositions can be achieved using top-down techniques but it is challenging and relies on complex tools or processes that are often expensive, energy intensive, and/or not environmentally benign.[2,3] Liquid metal nanoparticles have been made by dividing a macroscopic drop of liquid metal using ultrasonic scissioning in the presence of a stabilizer, though this technique can take several hours.[4,5] Liquid metal marbles and liquid metal/metal oxide frameworks made by coating liquid metal droplets with metal oxides, Teflon, silica, or carbon nanotube films are another method to make functional metal particles.[6,7] Microparticles of metal and metal alloys have been created using the droplet emulsion technique (DET) by shearing a molten metal in the presence of a carrier fluid.[8−10] Few researchers have utilized the DET to produce particles from room temperature liquid metals, like eutectic gallium–indium (EGaIn), that are gaining popularity in molecular electronics or to produce multicomponent particles for display devices, sensors, and self-assembly applications. This article reports a method for preparing micro- and nanoparticles by shearing liquids into complex particles (SLICE), an extension of the DET (Figure 1). The SLICE approach couples mechanical and chemical principles to create core–shell, hard or soft, smooth or patchy, micro- and nanoparticles and self-assembly principles postsynthesis to create unique assembled structures. We demonstrate our approach using low melting point metal alloys, which we break up to small sized particles under fluid flow with concomitant surface oxidation and functionalization.

Since compressible bodies evolve during flow to minimize their surface area (energy), it follows that control of shearing speed and felicitous choice of the shearing liquid ($\Delta P \approx$ W limit) can, potentially, lead to particles of different sizes and/or shapes.[10] We, therefore, hypothesized that using fluidic flow (Figure 1), *in situ* oxidation, and surface functionalization of the oxide surface, we can synthesize stable three-layered EGaIn (EGaIn = eutectic gallium–indium −75% Ga, 24.5% In w/w, mp ∼15.7 °C)[11] micro- and nanoparticles. Figure 1C gives a schematic illustration of structure of the proposed particles bearing a liquid metal core and a thin oxide layer functionalized with acetate.

EXPERIMENTAL SECTION

Materials. Glacial acetic acid (Pharmco-AAPER, ACS reagent grade 99.7%) was diluted in deionized water to make a 5% (v/v) solution. Trifluoroacetic acid (Alfa Aesar, 99%) was diluted in deionized water to make a 5% (v/v) solution. Gallium–indium eutectic (Aldrich, ≥99.99% trace metal basis) and bismuth indium tin ingot (Field's metal Bi:In:Sn 32.5/51/16.5 wt %, Alfa Aesar) were used

Received: September 2, 2014
Revised: October 30, 2014
Published: November 5, 2014

   dx.doi.org/10.1021/la5035118 | *Langmuir* 2014, 30, 14308−14313

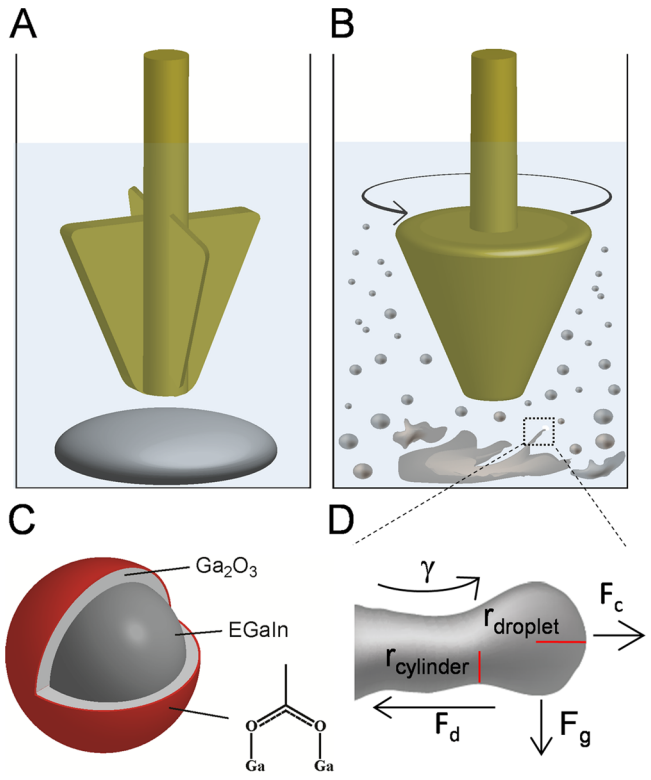

Figure 1. Schematic illustration of the SLICE process showing transformation of liquid metal, EGaIn, into micro- and nanoparticles. (A) Before being subjected to SLICE the two immiscible liquids are separate. (B) EGaIn while being sheared into micro- and nanoparticles. (C) Illustration of the architecture of the resulting liquid metal particle. (D) Illustration of the behavior of the liquid metal near the Rayleigh–Plateau limit where the stretched liquid breaks up into droplets; shear (γ), gravity (F_g), drag (F_d), centrifugal forces (F_c), buoyancy (F_b), and radius (r).

as received. Distilled white vinegar (Essential Everyday, 5% acidity, purchased from Shaw's supermarket) was used as received. Ethanol (Pharmco-AAPER, 200 proof anhydrous) and diethylene glycol (Sigma-Aldrich, 99%) were used as received. Undoped silicon wafers were diced, sonicated in acetone, and then dried in a filtered nitrogen stream to be used as substrates for electron microscopy.

Shearing Apparatus. A Dremel 3000 variable speed rotary tool with extender accessory was used as the shearing apparatus. The tool was operated at its maximum speed setting while its supply voltage was adjusted by a variable transformer in order to vary the rotational speed of the shearing implement. The shearing implement used was cross-shaped polytetrafluoroethylene (PTFE) with a steel rod core (Supporting Information, Figure S1).

A Signature Gourmet blender model SB-19 was also used as a shearing apparatus (Supporting Information, Figure S6). The model used has a 16 oz plastic cup. The tool was operated at its single speed setting while its supply voltage was adjusted to 110 V by a variable transformer and operated at 17 700 rpm.

Particle Creation. Rotary tool, EGaIn particles: A 5 mL aliquot of 5% acetic acid (or trifluoroacetic) in deionized water was placed into a flat-top glass vial with a 19 mm outer diameter and 50 mm height. A 0.6 g droplet of gallium–indium eutectic was directly added to the acetic acid solution. The gallium–indium eutectic was sheared at 20 °C using a PTFE shearing implement. Rotational speeds were varied between 5300 and 11 600 rpm using a variable transformer. Shearing time was varied from 5 to 30 min. The resulting suspension was allowed to sediment for 5–10 min, and the resulting supernatant was collected, diluted in ethanol 8×, drop-cast on silicon, dried, and analyzed by scanning electron microscopy.

Rotary tool, Field's metal particles: A 10 mL aliquot of 5% acetic acid in deionized water or diethylene glycol was placed into a 4 dram screw-top glass vial with a 28 mm outer diameter and 57 mm height. A 1.1 g of molten bismuth indium tin was directly added to the solution. The experiment was heated in an oil bath to 95 or 160 °C. The metal was melted at these temperatures. The liquid bismuth indium tin metal was sheared using a PTFE shearing implement. The PTFE shearing implement was rotated at 11 600 rpm. Shearing time was varied from 5 to 20 min. The experiment was removed from the hot oil bath, and PTFE shearing implement was slowed to a stop over 1 min. The resulting suspension was allowed to sediment for 5–10 min, and the resulting precipitate was collected, diluted in ethanol 8×, drop-cast on silicon, dried, and analyzed by scanning electron microscopy.

Blender, EGaIn particles: A 75 mL aliquot of distilled white vinegar was placed into the blender's 16 oz plastic cup. Approximately 1.1 g of gallium–indium eutectic was directly added to the liquid in the cup. The gallium–indium eutectic was sheared in the blender with a variable transformer setting of 110 V with a speed of 17 700 rpm. Total shearing time was 1 min. The resulting suspension was collected, diluted in ethanol 8×, drop-cast on silicon, let dry, and then analyzed by scanning electron microscopy.

RESULTS AND DISCUSSION

Under the SLICE approach to particle synthesis, forces acting on a liquid metal droplet include the following: shear (γ), gravity (F_g), drag (F_d), centrifugal forces (F_c), and buoyancy (F_b, a minor contributor due to density differences) (Figure 1D). For a body immersed in a moving fluid, the nature and intensity of interactions vary with respect to its intrinsic properties and its position around the flowing fluidic body. Initially, at $t = 0$, i.e., a stationary drop in the presence of a moving fluid (Figure 1A), γ dominates and stretches the drop into a cylinder-like shape, characterized by period wave-like instabilities (Figure 1D). On reaching the Rayleigh–Plateau limit (where radius $r_{droplet} > 1.5\ r_{cylinder}$), the cylindrical liquid metal breaks into droplets (Figure 1B).[12] Once the droplet is formed, a combination of F_d, F_c, and γ will ultimately split the droplet (work done on the droplet) until a final limit is attained where no more work is being done on the droplet ($\delta W = 0$). At this mechanical limit, forces acting on the droplet equal the Laplace pressure ($W = \Delta P$) and are directly proportional to the interfacial surface tension, γ_{int}, between the two liquids and the mean curvature, H (hence size for spheres), of the droplet (eq 1).

$$\Delta P = P_{droplet} - P_{fluid} = 2H\gamma_{int} \quad (1)$$

Here, $P_{droplet}$ and P_{fluid} are the pressure in the droplet and the shearing fluid, respectively. As the droplet gets smaller, F_d becomes a more dominant force. Drag force, which can be expressed in terms of drag coefficient C_d, is proportional to the relative rate of momentum transported by the fluid (eq 2).

$$C_d = \frac{2F_d}{A\rho V^2} \quad (2)$$

Here, A is the cross-sectional area of the body normal to the velocity vector, V is the velocity of the fluid, and ρ is the density of the fluid.

Since compressible bodies evolve during flow to minimize their surface area (energy), it follows that control of shearing speed and felicitous choice of the shearing liquid ($\Delta P \approx W$ limit) can, potentially, lead to particles of different sizes and/or shapes. We, therefore, hypothesized that, by using fluidic flow (Figure 1), *in situ* oxidation, and self-assembly on the oxide surface, we can synthesize stable three-layered EGaIn (EGaIn =

dx.doi.org/10.1021/la5035118 | *Langmuir* 2014, 30, 14308–14313

eutectic gallium−indium, 75% Ga, 24.5% In w/w, mp ∼15.7 °C)[11] micro- and nanoparticles. Figure 1C gives a schematic illustration of structure of the proposed particles bearing a liquid metal core and a thin oxide layer functionalized with acetate.

First, we synthesized EGaIn particles stabilized with a thin oxide layer shell in the presence of aqueous acetic acid. Most metals readily oxidize under ambient conditions forming a protective layer,[13] and the oxide of EGaIn is on the order of 0.7 nm.[14] This reactivity with air implies that nanoparticles delivered from such reactive metals can be further stabilized by modification of the oxide surface, in this case with acetate. A small quantity (0.6 g) of EGaIn was placed in 5% (v/v) acetic acid solution and sheared at 11 600 rpm for 20 min (Figure 1A). Detailed methods and materials can be found in the Supporting Information along with a picture of the shear apparatus (Supporting Information Figure S1). With increased shearing time, the solution turned from clear to a cloudy gray suspension with concomitant breakdown of the metal and increase in Tyndall scattering that gradually decreases as the particles settled (Supporting Information Figures S2 and S3) yielding a 2 mg/mL suspension of particles. Imaging by optical microscopy and electron microscopy (SEM and TEM) showed free and/or self-assembled spherical particles on the micrometer and nanometer size scale (Figure 2). Capillary-driven

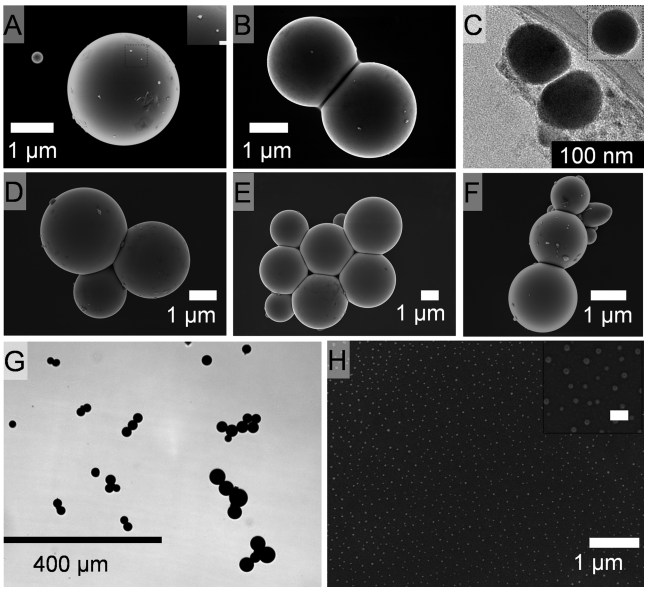

Figure 2. Images of shear generated EGaIn particles. (A) SEM image of micro- and nanoparticles, insert scale bar is 100 nm. Assembled particle dimers visualized by SEM (B) and TEM (C), insert in part C shows a single particle by TEM. (D−F) Other complex arrangements realized through capillary driven self-assembly. (G) Light microscopy images of various microparticle assemblies. (H) Nanoparticles made using a blender, inset scale bar is 100 nm.

self-assemblies of the particles gave dimers (Figure 2B), trimer clusters (Figure 2C), and other complex structures (Figure 2E−G). Small particles (43 and 52 nm for insert Figure 2A) were observed alongside larger particles. Average particle sizes calculated from SEM images were 1.14 ± 1.90 μm, a polydisperse distribution of particle sizes. It is unclear from SEM alone if the assemblies are groups of particles or a larger particle formed by the coalescence of smaller particles.

Particles made from EGaIn show properties of a malleable material. As observed on the microscale, aggregated particles appear flat on the surfaces where particles are in contact (Figure 2B−G). This is different from general particle aggregation because there is a force pulling these particles together and deforming into chains and into regular packing with flat edges where they touch. These flat sections, at the very least, suggest the particles are deformable but not necessarily composed of a liquid metal. Using energy-dispersive X-ray spectroscopy (EDS), composition of these microparticles was determined to be 74% gallium and 26% indium which match the bulk metal alloy within error (see Supporting Information Figure S4). Within the limitation of transmission electron microscopy (TEM) the interior of particles with diameters 4.8 μm to 6.4 nm were imaged (Supporting Information Figure S5). As shown by SEM for microparticles (Figure 2B), dimers of nanoparticles were also observed under TEM (Figure 2C) with a 1.2 nm gap between them: the inset shows a round nanoparticle (diameter of 85.5 nm). We infer that capillary forces during the drying process induce self-assembly, and though the forces were strong enough to deform the particles on contact, it was not enough to break the surface layers and cause the particles to coalesce (Figure 2C).

Since all particles were made in the presence of air and water, a thin film of predominantly Ga_2O_3 is expected to form on the surface of the liquid metal. Surface characterization using X-ray photoelectron spectroscopy (XPS) on bulk EGaIn without acid and EGaIn particles made in the presence of trifluoracetic acid confirm the presence of gallium oxide in both cases by presence of a Ga 3d peak at 20.9 and 21.1 eV, respectively. Elemental gallium was also confirmed by the presence of a Ga 3d peak at 18.8 eV for both bulk EGaIn and EGaIn particles. Acetic acid can bind to the oxide to form an outer organic layer on the particles. XPS of EGaIn particles, made with acetic acid being replaced with trifluoroacetic acid, indicates that the acetate is present and chemically binding to the surface of the particles giving an organic outer layer (see Supporting Information Figure S4 and Table S1). This implies at least two layers composed of an acetate bound on an oxide.[15] Similarly, we subjected EGaIn to a blender with distilled white vinegar as the shearing fluid (Supporting Information Figure S6). Imaging by SEM revealed a large field of nanoparticles that were 31.3 ± 6.1 nm in diameter (Figure 2H) and also larger microparticles (Supporting Information Figure S6). The speed of the blender (17 700 rpm) is signification faster than the dremel tool (11 600 rpm) and with a larger diameter of 42 mm compared to 13 mm. These differences account for the higher shear force (γ) the EGaIn experiences and hence the smaller end particle size.

Imaging, surface, and EDS analysis of the EGaIn particles clearly show a core−shell particle but give no definitive evidence of the phase of the core. To establish if the particles have a liquid core, removing the two outer layers of a particle dimer, such as in Figure 2B, should allow the two cores to touch and coalesce if they are in fact liquid. A liquid core would infer that these particles are reconfigurable postsynthesis, and when coupled with self-assembly seen above (Figure 1B−F), postsynthetic modification would give otherwise unattainable complex structures. A focused ion beam (FIB) of gallium ions was used to gently mill away a rectangular area over a particle dimer with periodic imaging by SEM (Figure 3A). The initial surface of the two particles has a smooth texture highlighted in blue (for noncolorized version see Supporting Information Figure S7). As the particles are milled, the top two layers are

dx.doi.org/10.1021/la5035118 | *Langmuir* 2014, 30, 14308−14313

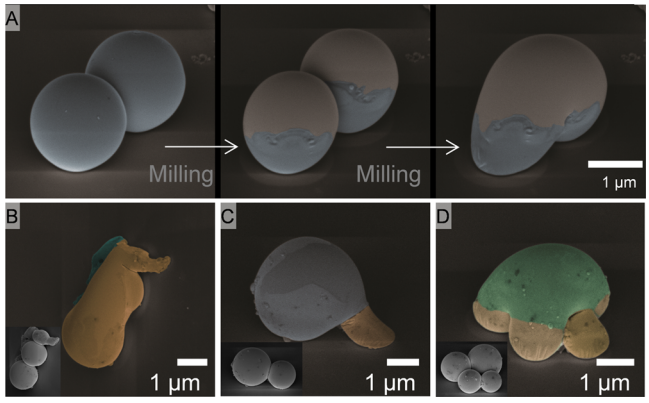

Figure 3. Milling outer surface layers of EGaIn particles to expose the liquid core using FIB gives complex structures and demonstrates reconfigurable nature of these particles. (A) A dimeric assembly is slowly milled to remove the outer organic and oxide layers until dimer merges. (B–D) Clusters of assemblies (inserts) milled into the shape of a seahorse (B), cap (C), and turtle (D).

removed revealing two smooth surfaces (Figure 3Aii) that, upon further milling, coalesce to form one nonspherical particle indicating flow, a defining property of fluids. Because the surface layers on the underside are shadowed by the top portion of the particles, the intact oxide/organic layers hold part of the liquid EGaIn in place while the bare top portion of the EGaIn coalesces. In the evacuated environment of the SEM, there is no water or oxygen to reform the oxide shell. Figure 3B–D shows other assemblies bearing particles of different sizes or shapes (inserts) that were milled into complex structures like a seahorse (Figure 3B), a cap (Figure 3C), and a turtle (Figure 3D).

The Lowengrub–Voigt model on behavior of multicomponent drops under fluidic flow predicts that the surface composition would either evolve to phase-segregate or, at the least, be dynamic giving random compositions.[16] This model predicts that as a drop deforms under shear, the component with smallest surface tension should accumulate on the drop tip where the curvature is largest.[16,17] We, therefore, hypothesized that, under SLICE, surface tension driven phase segregation occurs. When low melting solids are subjected to SLICE, therefore, any differences in surface composition can be retained upon solidification to give particles with variable surface composition and/or morphologies.

Field's metal (Bi 32.5%, In 51%, Sn 16.5%, mp 62 °C), when heated above its melting point, can be subjected to SLICE using conditions similar to the preparation of EGaIn particles. Field's metal was heated in an aqueous 5% acetic acid solution to 95 °C and sheared at 11 600 rpm into fine particles over 20 min, then slowly cooled to room temperature while stirring. The yield was a 170 μg/mL suspension of fine particles. These fine suspensions slowly settled over time in a manner similar to the EGaIn particles. Large quantities of microparticles were observed under a light microscope (Figure 4A, Supporting Information Figure S8) and homogeneous looking nano-

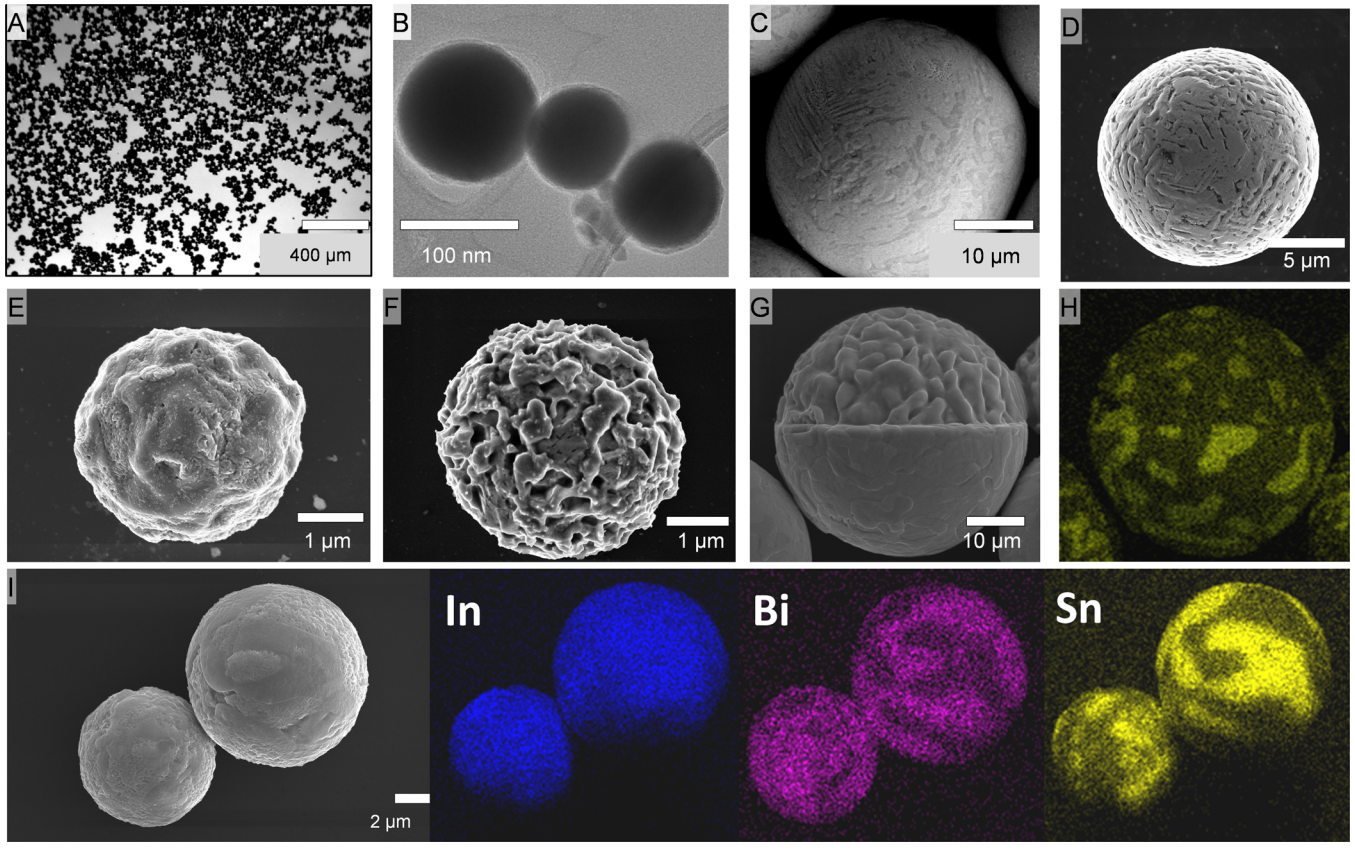

Figure 4. Application of SLICE in the synthesis of particles with varied morphologies from Field's metal melts. (A) Microscope image of a large number of microparticles. (B) TEM images of metal nanoparticles. (C–F) Particles of different surface morphologies and compositions. (G) A partially milled particle. (H) Elemental mapping of partially milled particle (in G). (I) A particle with well-defined phase segregated regions and EDS elemental mapping of the particles.

dx.doi.org/10.1021/la5035118 | *Langmuir* 2014, 30, 14308–14313

particles were observed by TEM (Figure 4B). Average particle sizes measured by SEM were 12.6 ± 8.9 μm.

Applying the Lowengrub−Vogt model to Field's metal melt, (surface energy of the components; γ_{sn} = 0.49 J/m^2, $\gamma_{In} \approx \gamma_{Bi}$ = 0.68 J/m^2)[18] suggests that Sn would preferentially phase segregate to the surface when a drop of the melt is subjected to shear stress under fluidic flow. Differences in density (ρ_{Sn} = 7.27 g/cm^3, ρ_{In} = 7.31 g/cm^3, ρ_{Bi} = 9.79 g/cm^3), however, suggest that Bi would precipitate under gravitational and centrifugal forces. When Field's metal melts were subjected to SLICE, two phase segregated domains on the surface of the particles were observed (Figure 4E). Belts of a smooth top layer partially cover the surface of the particle, while below it a rougher layer is observed. Elemental mapping reveals the two phase segregated regions as Bi and Sn rich with indium being evenly distributed throughout the particles. These results suggest that density and surface tension, as predicted, are important variables in creating particles of varied surface compositions using SLICE. The presence of Sn, instead of only the heavier Bi, on the outer surface of the particles supports the Lowengrub−Vogt model and further demonstrates the applicability of fluid dynamics in creating complex structures.

When two metals phase segregate out of ternary systems and these metals have different coefficient of linear expansion (α_{Sn} = 22 × 10^{-6} K^{-1}, α_{Bi} = 13.4 × 10^{-6} K^{-1}) and reactivity, the resulting surface is unlikely to be smooth. The phase-segregated particles showed various surface morphologies by SEM (Figure 4). We observed round particles with the following: lamellar type texture (Figure 4C) (formed by shearing in a 5% acetic acid solution in diethylene glycol at 11 600 rpm for 20 min),[19] smooth woven texture, "surface rods" (Figure 4D), bumpy surfaces (Figure 4E), rough porous surfaces (Figure 4F), and patches of alternating swirls of smooth and rough textures (Figure 4I).

Internal phase separation was probed by partially milling half of a particle (Figure 4G) followed by elemental mapping of the whole particle (Figure 4H) and imaging using energy selective backscattered (EsB) detector (Supporting Information Figure S9). As expected, phase separated Sn can also be seen in the core of these particles but in smaller patches and in patterns that do not mirror the enrichment observed on the surface. The striation (Figure 4C), porosity (Figure 4D), or the lamellar type (Figure 4E) patterns were not observed in the core of the particles, but as expected, random enrichment of one metal over the others was observed indicating that the patterns observed on the surface of the particles are due to a surface phenomenon. We infer that SLICE can be used to engineer surface composition, an important parameter in applications such as catalysis.

CONCLUSION

We demonstrate a low-cost, green, and facile approach to nano- and microparticle synthesis. First, we fabricated soft-core−shell nanoparticles by shearing a liquid metal, oxidizing the most reactive metal with concomitant *in situ* stabilization using a surface attached carboxylic acid. The particles generated from room temperature liquid metals were modified after synthesis to give new particles bearing complex shapes. Melts were also used to generate particles with tunable surface composition or surface morphology. Using surface tension under fluidic flow and density differences to induce phase separation, we generated particles with different surface morphologies and compositions. Previously, patchy particles were difficult to make. By using SLICE, however, we rapidly synthesize patchy particles and at low cost. Our results show that SLICE is a simple, versatile method that can be fine-tuned to realize particles of various sizes, shapes, compositions and surface morphologies.

ASSOCIATED CONTENT

Supporting Information

Details concerning instrumentation. This material is available free of charge via the Internet at http://pubs.acs.org.

AUTHOR INFORMATION

Corresponding Author

*E-mail: mthuo@iastate.edu.

Author Contributions

The manuscript was written through contributions of all authors. All authors have given approval to the final version of the manuscript.

Notes

The authors declare no competing financial interest.

ACKNOWLEDGMENTS

We thank Mathieu Gonidec for technical assistance, and thank Luna E. Rafael of Luna Scientific Storytelling Inc. for help with the manuscript. This work was supported by the Iowa State University and University of Massachusetts—Boston through startup funds.

REFERENCES

(1) Bonnemann, H.; Richards, R. M. Nanoscopic Metal Particles—Synthetic Methods and Potential Applications. *Eur. J. Inorg. Chem.* **2001**, *10*, 2455−2480.

(2) Hyun, D. C.; Levinson, N. S.; Jeong, U.; Xia, Y. Emerging Application of Phase-change Materials (PCMs): Teaching an Old Dog New Tricks. *Angew. Chem., Int. Ed.* **2014**, *53*, 3780−3795.

(3) Wiley, B.; Sun, Y.; Xia, Y. Synthesis of Silver Nanostructures with Controlled Shapes and Properties. *Acc. Chem. Res.* **2007**, *40* (10), 1067−1076.

(4) Hohman, J. N.; Kim, M.; Wadsworth, G. A.; Bednar, H. R.; Jiang, J.; LeThai, M. A.; Weiss, P. S. Directing Substrate Morphology via Self-Assembly: Ligand-Mediated Scission of Gallium-Indium Microspheres to the Nanoscale. *Nano Lett.* **2011**, *11* (12), 5104−5110.

(5) Han, Z. H.; Yang, B.; Qi, Y.; Cumings, J. Synthesis of Low-Melting-Point Metallic Nanoparticles with an Ultrasonic Nano-emulsion Method. *Ultrasonics* **2011**, *51* (4), 485−488.

(6) Sivan, V.; Tang, S.-Y.; O'Mullane, A. P.; Petersen, P.; Eshtiaghi, N.; Kalantar-zadeh, K.; Mitchell, A. Liquid Metal Marbles. *Adv. Funct. Mater.* **2013**, *23* (2), 144−152.

(7) Zhang, W.; Ou, J. Z.; Tang, S.-Y.; Sivan, V.; Yao, D. D.; Latham, K.; Khoshmanesh, K.; Mitchell, A.; O'Mullane, A. P.; Kalantar-zadeh, K. Liquid Metal/Metal Oxide Frameworks. *Adv. Funct. Mater.* **2014**, *24* (24), 3799−3807.

(8) Allen, W. P.; Perepezko, J. H. Solidification of Undercooled Sn-Sb Peritectic Alloys. 1. Microstructural Evolution. *Metall. Trans. A* **1991**, *22* (3), 753−764.

(9) Perepezko, J. H.; Sebright, J. L.; Hockel, P. G.; Wilde, G. Undercooling and Solidification of Atomized Liquid Droplets. *Mater. Sci. Eng., A* **2002**, *326* (1), 144−153.

(10) Wang, Y. L.; Xia, Y. N. Bottom-up and Top-down Approaches to the Synthesis of Monodispersed Spherical Colloids of Low Melting-point Metals. *Nano Lett.* **2004**, *4* (10), 2047−2050.

(11) Dickey, M. D.; Chiechi, R. C.; Larsen, R. J.; Weiss, E. A.; Weitz, D. A.; Whitesides, G. M. Eutectic Gallium-indium (EGaIn): A Liquid Metal Alloy for the Formation of Stable Structures in Microchannels at Room Temperature. *Adv. Funct. Mater.* **2008**, *18* (7), 1097−1104.

(12) de Gennes, P.-G.; Brochard-Wyart, F.; Quere, D. *Capillarity and Wetting Phenomena Drops, Bubbles, Pearls, Waves*; Springer: New York, 2004.
(13) Xu, Q.; Oudalov, N.; Guo, Q.; Jaeger, H. M.; Brown, E. Effect of Oxidation on the Mechanical Properties of Liquid Gallium and Eutectic Gallium-Indium. *Phys. Fluids* **2012**, *24* (6).
(14) Cademartiri, L.; Thuo, M. M.; Nijhuis, C. A.; Reus, W. F.; Tricard, S.; Barber, J. R.; Sodhi, R. N. S.; Brodersen, P.; Kim, C.; Chiechi, R. C.; Whitesides, G. M. Electrical Resistance of AgTS-S(CH2)n-1CH3//Ga2O3/EGaIn Tunneling Junctions. *J. Phys. Chem. C* **2012**, *116* (20), 10848−10860.
(15) de Silva, C. M.; Pandey, B.; Ito, T. Adsorption of Primary Substituted Hydrocarbons onto Solid Gallium Substrates. *Langmuir* **2013**, *29*, 4568−4573.
(16) Lowengrub, J. S.; Xu, J.-J.; Voigt, A. Surface Phase Separation and Flow in a Simple Model of Multicomponent Drops and Vesicles. *Fluid Dynam. Mater. Process.* **2007**, *13* (1), 1−19.
(17) Ferrando, R.; Jellinek, J.; Johnston, R. L. Nanoalloys: From Theory to Applications of Alloy Clusters and Nanoparticles. *Chem. Rev.* **2008**, *108* (3), 845−910.
(18) Vitos, L.; Ruban, A. V.; Skriver, H. L.; Kollar, J. The Surface Energy of Metals. *Surf. Sci.* **1998**, *411* (1-2), 186−202.
(19) Sengupta, S.; Soda, H.; McLean, A. Evolution of Microstructure in Bismuth-Indium-Tin Eutectic Alloy. *J. Mater. Sci.* **2005**, *40* (9-10), 2607−2610.